Kinetic and electron paramagnetic resonance studies on radical polymerization. Radical copolymerization of *p-tert*-butoxystyrene and dibutyl fumarate in benzene

Tsuneyuki Sato, Sumio Shimooka, Makiko Seno, Hitoshi Tanaka*

Department of Chemical Science and Technology, Faculty of Engineering, Tokushima University, Minamijosanjima 2-1, Tokushima 770, Japan

(Received: January 19, 1993; revised manuscript of July 9, 1993)

SUMMARY:

The copolymerization of *p-tert*-butoxystyrene (**1**) (M_1) and dibutyl fumarate (**2**) (M_2) initiated with dimethyl 2,2'-azobisisobutyrate (**3**) was studied in benzene at 60 °C kinetically and by means of electron paramagnetic resonance (EPR) spectroscopy. The monomer reactivity ratios were determined to be r_1 = 0,18 and r_2 = 0,01, indicating that homopropagation of M_2 is almost negligible in the copolymerization. The copolymerization system was revealed to involve EPR-observable propagating polymer radicals under practical copolymerization conditions. The apparent rate constants of propagation (k_p) and termination (k_t) determined by EPR show a rapid increase in the range from 0,9 to 1,0 of feed composition (f_1 = {[M_1]/([M_1] + [M_2])}) of M_1. From the relationship between k_p and f_1 based on Fukuda's penultimate model, the rate constants of propagation of copolymerization were evaluated; k_{111} = 140 L · mol^{-1} · s^{-1}, k_{211} = 4,3 L · mol^{-1} · s^{-1}, k_{112} = 778 L · mol^{-1} · s^{-1}, k_{212} = 24 L · mol^{-1} · s^{-1} and k_{121} = 19 L · mol^{-1} · s^{-1}, suggesting a pronounced penultimate effect.

Introduction

Recently much attention has been paid to the penultimate effect in the kinetics of free radical copolymerizations[1–6]. From the rate constants of propagation and termination determined by using the rotating sector method, Fukuda et al. concluded that any abnormal effects in the copolymerization kinetics are related to the propagation and not to the termination reaction[1]. The copolymerization results by O'Driscoll et al. using a pulsed laser technique also led the same conclusion[7].

In the previous papers we reported on kinetic and electron paramagnetic resonance (EPR) spectroscopic evidences for the penultimate effect in the copolymerization of *N*-cyclohexylmaleimide and dialkyl itaconates[8,9].

More recently we have found that the copolymerization system of *p-tert*-butoxystyrene (**1**) and dibutyl fumarate (**2**) involves EPR-observable propagating polymer

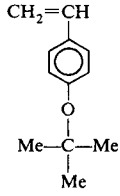

1

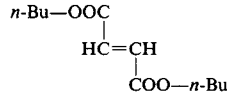

2

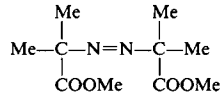

3

 CCC 1022-1352/94/$08.00

radicals under the actual copolymerization conditions and the penultimate unit of **2** exerts a marked effect on the reactivity of propagating radical end derived from **1**.

The present paper deals with the results of kinetic and EPR studies on the copolymerization of **1** and **2** initiated with dimethyl 2,2'-azobisisobutyrate (**3**) in benzene at 60 °C.

Experimental part

p-tert-Butoxystyrene (**1**) (from Hokko Chemical Industry Co., Ltd.) and dibutyl fumarate (**2**) (from Tokyo Kasei Kogyo Co., Ltd.) were washed by a 5% aqueous NaOH solution, dried over sodium sulfate and distilled. Dimethyl 2,2'-azoisobutyrate (**3**) (from Wako Pure Chemical Industries) was used after recrystallization from methanol. Benzene was purified by the usual method.

Polymerization and copolymerization of **1** and **2** initiated with **3** were carried out in a degassed and sealed tube at 60 °C. After a given time the polymerization mixture was poured into a large amount of methanol to isolate the polymer. The resulting polymer was filtered off, dried i. vac. and weighed. The composition of copolymer was established from the carbon content by elemental analysis.

Gel-permeation chromatograms (GPC) were recorded at 38 °C by using a TOSO-HLC 802A instrument with tetrahydrofuran as eluent. From the GPC results, the number- and weight-average molecular weights ($\bar{M}_n$ and $\bar{M}_w$) were estimated by standard procedures using polystyrene standards. EPR spectra of the copolymerization mixtures in a degassed and sealed EPR tube were recorded on a JEOL-JES-FG2XG spectrometer operating at X-band (9,5 GHz) with a TE mode cavity.

Results and discussion

Copolymerization of **1** *and* **2** *with* **3**

The copolymerization of **1** (M_1) and **2** (M_2) using **3** as initiator was performed in benzene at 60 °C. The total concentration of **1** and **2** was kept constant at 3,00 mol · L^{-1}, and the concentration of **3** was fixed at 5,00 10^{-2} mol · L^{-1}. Tab. 1 summarizes the results of copolymerization.

Tab. 1. Radical copolymerization of **1** (M_1) andd **2** (M_2) initiated with **3** in benzene at 60 °C[a]

Content of M_1 in feed in mol-%	Yield in %	Carbon content in %[b]	Content of M_1 unit in copolymer in mol-%
10	7,0	70,9	48,2
20	5,8	71,0	48,7
30	5,7	71,0	48,7
50	9,5	71,8	53,1
70	8,0	72,8	58,4
80	8,6	73,8	63,5
90	9,5	75,6	72,5

[a] $[M_1] + [M_2] = 3{,}00$ mol · L^{-1}, $[3] = 5{,}00 \cdot 10^{-2}$ mol · L^{-1}.
[b] Determined by elemental analysis.

Fig. 1 shows the relationship between the copolymer composition and the feed composition $\{f_1 = [M_1]/([M_1] + [M_2])\}$ of **1**. The monomer reactivity ratios were estimated according to curve-fitting based on the nonlinear least-squares method as follows:

$$r_1 = 0{,}18 \qquad r_2 = 0{,}01$$

The Fineman-Ross method gave similar results ($r_1 = 0{,}18$, $r_2 = 0{,}03$). The solid line in Fig. 1 was obtained using the former values of r_1 and r_2. Thus the copolymerization shows such a high alternating tendency that alternating copolymer is yielded in the feed composition range of f_1 less than 0,5 and that monomer **2** hardly adds to a polymer radical bearing the same terminal unit.

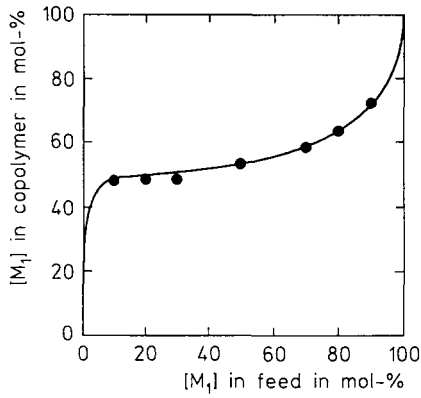

Fig. 1.

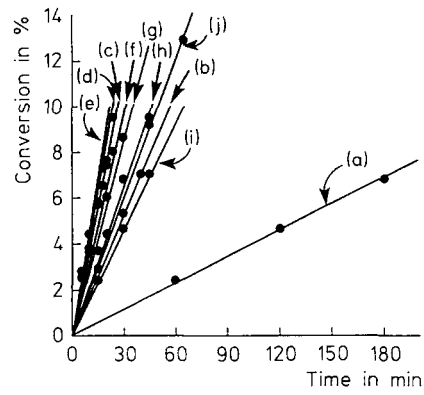

Fig. 2.

Fig. 1. *Copolymer composition curve in the copolymerization of* **1** (M_1) *and* **2** (M_2) *initiated with* **3** *in benzene at* 60 °C. [**1**] + [**2**] = 3,00 mol · L^{-1}, [**3**] = 5,00 · 10^{-2} mol · L^{-1}

Fig. 2. Time-conversion plots in the copolymerization of **1** and **2** initiated with **3** in benzene at 60 °C . [**1**] + [**2**] = 3,00 mol · L^{-1}, [**3**] = 5,00 · 10^{-2} mol · L^{-1}. [**1**]/([**1**] + [**2**]) = (a) 0, (b) 0,1, (c) 0,2, (d) 0,3, (e) 0,5, (f) 0,7, (g) 0,8, (h) 0,9, (i) 1,0, (j) 1,0 in bulk ([**1**] = 5,21 mol · L^{-1})

Fig. 2 presents the time-conversion plots observed in the copolymerization. From the slopes of the plots and the composition of the resulting copolymers, the rates of copolymerization (R_p) were calculated. They are listed in Tab. 2, together with the molecular weights of copolymers. Fig. 3 shows the relation of R_p with f_1. R_p shows a broad maximum near $f_1 = 0{,}4$.

Determination of apparent rate constants of propagation (k_p) and termination (k_t) in the copolymerization by means of EPR

The copolymerization system of **1** and **2** was found to involve EPR-observable propagating radicals under the actual copolymerization conditions. Fig. 4 shows EPR spectra observed at different monomer feed compositions. The EPR spectra were easily

Tab. 2. Copolymerization rate (R_p) and molecular weight of copolymer in the copolymerization of **1** (M_1) and **2** (M_2) initiated with **3** in benzene at 60 °C[a]

$\frac{[M_1]}{[M_1] + [M_2]}$	$10^4 \cdot R_p$ / mol · L^{-1} · s^{-1}	$10^{-5} \cdot \bar{M}_n$	$10^{-5} \cdot \bar{M}_w$	$\bar{M}_w/\bar{M}_n$
0	0,192	0,11	0,19	1,7
0,1	0,981	1,00	1,89	1,9
0,2	2,01	1,22	2,25	1,9
0,3	2,09	1,45	2,87	2,0
0,5	2,04	1,47	3,19	2,2
0,7	1,70	1,42	3,17	2,2
0,8	1,45	0,96	1,89	2,0
0,9	1,03	0,87	1,55	1,8
1,0	0,778	0,65	1,12	1,7
1,0[b]	1,68	1,52	2,62	1,7

a) [1] + [2] = 3,00 mol · L^{-1}, [3] = 5,00 · 10^{-2} mol · L^{-1}.
b) In the polymerization of **1** in bulk; ([1] = 5,21 mol · L^{-1}).

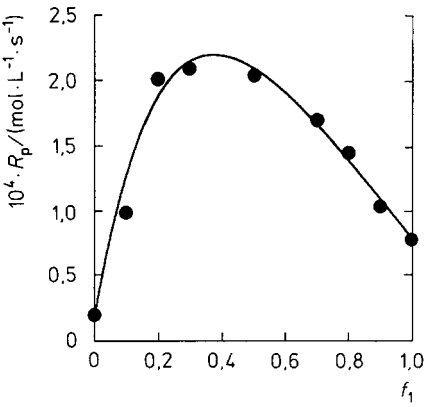

Fig. 3. Relationship between the copolymerization rate (R_p) and f_1 ([1]/([1] + [2])) in benzene at 60 °C. [1] + [2] = 3,00 mol · L^{-1}, [3] = 5,00 · 10^{-2} mol · L^{-1}

measurable even at high relative concentrations of **1** up to f_1 = 0,9, while the concentration of propagating poly(**1**) radical, **4**, was very low in the homopolymerization of **1**. Spectrum (a) observed in the homopolymerization of **2** is due to propagating radical **5** of **2**. A similar spectrum has been reported for the propagating polymer radical of diisopropyl fumarate[10]. A four-line spectrum (i) is assignable to polymer radical **4**. A

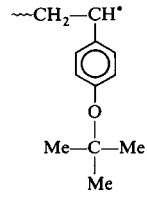

4

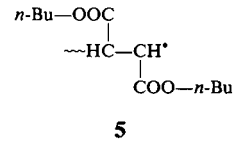

5

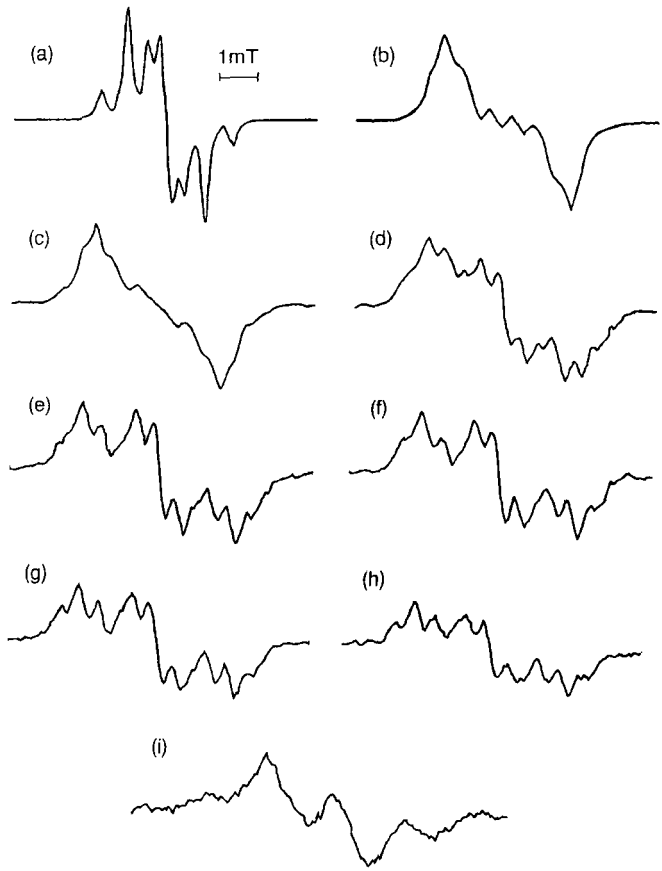

Fig. 4. EPR spectra of the **1/2/3** system in benzene at 60 °C. [**1**] + [**2**] = 3,00 mol · L^{-1}, [**3**] = 5,00 · 10^{-2} mol · L^{-1}. [**1**]/([**1**] + [**2**]) = (a) 0, (b) 0,1, (c) 0,2, (d) 0,3, (e) 0,5, (f) 0,7, (g) 0,8, (h) 0,9, (i) 1,0 in bulk at 80 °C

similar four-line spectrum has been reported for the propagating polymer radical in the bulk polymerization of styrene[11]. The spectrum of the copolymerization system was found to change with monomer feed composition, indicating that spectra (b)–(h) observed in the copolymerization system are due to mixtures of propagating polymer radicals **4** and **5**.

The total concentration ([P$^{\bullet}$]) of propagating radicals was determined at 60 °C by computer double integration of the observed EPR spectra, where 2,2′,6,6′-tetramethylpiperidinyloxy radical (TEMPO) in the same medium was used as reference. Tab. 3 summarizes the results thus determined which are expected to have an error of less than ±15%. The total concentration of polymer radicals decreased with increasing f_1. There is a large difference between [P$^{\bullet}$]'s at f_1 = 0,9 and at f_1 = 1,0.

Tab. 3. Total polymer radical concentration ([P•]), rate constants of propagation (k_p) and termination (k_t) and $k_d \cdot f$[a] in the copolymerization of **1** (M_1) and **2** (M_2) initiated with **3** at 60 °C in benzene[b]

$[M_1]$ / $[M_1] + [M_2]$	$10^6 \cdot [P^\bullet]$ / mol · L^{-1}	k_p[c] / L · mol^{-1} · s^{-1}	$10^6 \cdot k_d \cdot f$ / s^{-1}	$10^{-4} \cdot k_t$[d] / L · mol^{-1} · s^{-1}
0	62	0,10	4,0	0,010
0,1	24	1,4	4,1	0,071
0,2	11	6,1	4,2	0,35
0,3	7,5	9,3	4,4	0,78
0,5	5,3	13	4,6	1,6
0,7	4,0	14	5,0	3,3
0,8	3,5	14	5,0	4,9
0,9	2,3	15	5,2	9,8
1,0	0,18	140	5,5	1700
1,0[e]	0,23	140	5,5	1000

a) k_d: decomposition rate constant of **3**, f: initiator efficiency.
b) [**1**] + [**2**] = 3,00 mol · L^{-1}, [**3**] = 5,00 · 10^{-2} mol · L^{-1}.
c) Determined according to Eq. (1).
d) Determined according to Eq. (2).
e) In the polymerization of **1** in bulk; ([**1**] = 5,21 mol · L^{-1}).

Independently of termination, the k_p value could be directly calculated using R_p (Tab. 2) and [P•] (Tab. 3) according to Eq. (1):

$$R_p = k_p [P^\bullet] [M] \quad (1)$$

where [M] = [**1**] + [**2**]. The k_p values obtained are also included in Tab. 3 and are expected to have an error of less than ±20%. A large gap is observed in the k_p values at f_1 = 0,9 and f_1 = 1,0. k_p at f_1 = 0 (0,1 L · mol^{-1} · s^{-1}) corresponds the rate constants of propagation of **2** and is similar to that (0,058 L · mol^{-1} · s^{-1}) of dimethyl fumarate at 60 °C[12]. The very low k_p value conforms to the above conclusion obtained in the copolymerization that homopropagation of **2** is negligible in the present copolymerization system. k_p at f_1 = 1,0 (140 L · mol^{-1} · s^{-1}) is the rate constant of propagation of **1**, which was determined both in bulk and in a benzene solution of **1** (3,0 mol · L^{-1}). The rate constant of propagation for *p*-substituted styrenes is known to be reduced by electron-donating substituents[13]. The rate equation of propagation by O'Driscoll et al. gives 146 L · mol^{-1} · s^{-1} for *p*-methoxystyrene at 60 °C[7].

In order to elucidate the k_t value, the $k_d f$ value of **3** was determined under the copolymerization conditions by means of radical trapping with TEMPO in the same manner as described in the previous paper[8], where k_d is the rate constant of decomposition of **3** and f the initiator efficiency. **3** decomposes into 1-methyl-1-methoxycarbonylethyl radicals and nitrogen. Some of the primary radicals disappear through cage

reactions. The others diffuse through the solvent cage to initiate the copolymerization. When the decomposition of **3** is conducted in the presence of TEMPO, the primary radicals escaping from the solvent cage are trapped with TEMPO to yield a coupling product. Therefore the $k_d f$ value can be evaluated by following the decrease in the TEMPO concentration by means of EPR. Tab. 3 lists the $k_d f$ values determined at 60 °C for different monomer feed compositions. The $k_d f$ value decreases with decreasing f_1. This stems from reduction of the f value by viscosity effect due to the high-viscous monomer **2**.

Using $[P^\bullet]$ and $k_d f$, the k_t values (which seem to have an error of less than ±40%) were determined according to Eq. (2), and are presented in Tab. 3.

$$2\, k_d f\, [3] = k_t\, [P^\bullet]^2 \tag{2}$$

Thus, k_t increases with increasing f_1 and also shows a drastic increase at $f_1 = 1{,}0$. k_t of **2** (100 $L \cdot mol^{-1} \cdot s^{-1}$) is reasonably larger than that (17,5 $L \cdot mol^{-1} \cdot s^{-1}$) of diisopropyl fumarate at 60 °C reported[14]. k_t of **1** in bulk ($1{,}0 \cdot 10^7$ $L \cdot mol^{-1} \cdot s^{-1}$) seems to be properly smaller than that ($7{,}2 \cdot 10^7$ $L \cdot mol^{-1} \cdot s^{-1}$) of styrene at 60 °C in bulk[15].

Relationship between k_p and f_1

Fig. 5 shows the relationship between the apparent propagation rate constant and the monomer feed composition.

In the terminal model, the rate (R_p) of copolymerization of M_1 and M_2 is expressed by Eq. (3).

$$R_p = k_p\, [P^\bullet]\, [M] = k_{11}\, [P_1^\bullet]\, [M_1] + k_{12}\, [P_1^\bullet]\, [M_2] + k_{21}\, [P_2^\bullet]\, [M_1] + k_{22}\, [P_2^\bullet]\, [M_2] \tag{3}$$

where $P_1^\bullet$ = polymer radical of M_1, $P_2^\bullet$ = polymer radical of M_2, $[P^\bullet] = [P_1^\bullet] + [P_2^\bullet]$, $[M] = [M_1] + [M_2]$, and k_p = apparent rate constant of propagation.

When a stationary state is reached with respect to the propagating polymer radicals $P_1^\bullet$ and $P_2^\bullet$, Eq. (4) is valid:

$$k_{12}\, [P_1^\bullet]\, [M_2] = k_{21}\, [P_2^\bullet]\, [M_1] \tag{4}$$

Substitution of Eq. (4) into Eq. (3) yields Eq. (5).

$$R_p = k_{11}\, [P_1^\bullet]\, [M_1] + 2k_{12}\, [P_1^\bullet]\, [M_2] + k_{22}\, [P_2^\bullet]\, [M_2] \tag{5}$$

k_p is calculated using Eq. (6)[1], where $f_2 = 1 - f_1$.

$$k_p = (r_1 f_1 + 2 f_1 f_2 + r_2 f_2)/(r_1 f_1/k_{11} + r_2 f_2/k_{22}) \tag{6}$$

The dashed line in Fig. 5 represents the calculated k_p value. Thus, the observed k_p values are fairly higher than calculated ones in the lower f_1 region, while the reverse is

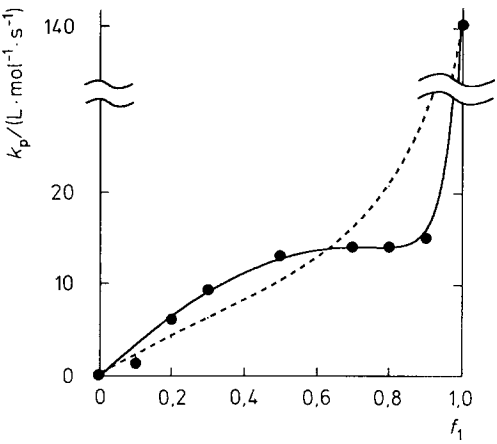

Fig. 5. Relationship between the apparent rate constant (k_p) and f_1 ([1]/([1] + [2])). The circles are observed values, and the dashed and solid lines represent the terminal and penultimate model predictions, respectively

observed in the higher f_1 region. Such deviations are ascribable to the penultimate effect. The above findings suggest that the reactivity of propagating radical **5** (derived from **2**) is enhanced by the penultimate **1** monomeric unit, whereas that of **4** (derived from **1**) is highly suppressed by the penultimate **2** monomeric unit.

We have attempted to evaluate the rate constant of each propagation step of the copolymerization in the following manner.

Since homopropagation of M_2 monomer is negligible in the present copolymerization, R_p is given by Eq. (7).

$$R_p = k_{11} [P_1^\bullet] [M_1] + 2k_{12} [P_1^\bullet] [M_2] \tag{7}$$

Using Eq. (4) and $[P^\bullet] = [P_1^\bullet] + [P_2^\bullet]$, we obtain Eqs. (8) and (9).

$$k_{12} [P_1^\bullet] [M_2] = k_{21} [M_1] ([P^\bullet] - [P_1^\bullet]) \tag{8}$$

$$[P_1^\bullet] = k_{21} [M_1] [P^\bullet]/(k_{12} [M_2] + k_{21} [M_1]) \tag{9}$$

When Eq. (9) is substituted into Eq. (7), R_p is presented by:

$$R_p = k_p [P^\bullet] [M] = k_{21} [P^\bullet] \{(k_{11} [M_1]^2 + 2k_{12} [M_1] [M_2])/(k_{21} [M_1] + k_{12} [M_2])\} \tag{10}$$

Then we obtain Eq. (11).

$$k_p [M] = k_{21} \{(k_{11} [M_1]^2 + 2k_{12} [M_1] [M_2])/(k_{21} [M_1] + k_{12} [M_2])\} \tag{11}$$

Putting $f_1 = [M_1]/[M]$ and $(1-f_1) = [M_2]/[M]$ into Eq. (11) yields Eq. (12).

$$\begin{aligned} k_p &= k_{21} \{k_{11} f_1^2 + 2k_{12} f_1 (1 - f_1)\}/\{k_{21} f_1 + k_{12} (1 - f_1)\} \\ &= k_{21} \{(k_{11} - 2k_{12}) f_1^2 + 2k_{12} f_1\}/\{(k_{21} - k_{12}) f_1 + k_{12}\} \end{aligned} \tag{12}$$

Substituting $k_{12} = k_{11}/r_1$ into Eq. (12) yields Eq. (13).

$$k_p = k_{21}\{(r_1 - 2)f_1^2 + 2f_1\}/\{(r_1 k_{21}/k_{11} - 1)f_1 + 1\} \quad (13)$$

Using the penultimate model of Fukuda et al.[1,16,17], where the ordinary monomer reactivity ratios, r_1 and r_2, are not affected by the penultimate unit, but the ratio $s = k_{211}/k_{111}$ differs from unity because of the penultimate effect, k_{11} is given by Eq. (14).

$$\begin{aligned} k_{11} &= k_{111}(r_1 f_1 + f_2)/(r_1 f_1 + s^{-1} f_2) \\ &= k_{111}\{(r_1 - 1)f_1 + 1\}/\{(r_1 - s^{-1})f_1 + s^{-1}\} \end{aligned} \quad (14)$$

where $r_1 = k_{111}/k_{112} = k_{211}/k_{212}$, and k_{lmn} is the rate constant for the addition of monomer n to the radical with a terminal unit m and a penultimate unit l (l, m, n = 1 or 2).

As described above, the copolymer composition curve of the present copolymerization is well represented by the terminal model, indicating that the monomer reactivity ratios are almost free from penultimate effect. Therefore the penultimate model is applicable to the present copolymerization system.

When Eq. (14) is substituted into Eq. (13), k_p is expressed by the parameters of r_1 (0,18), f_1, k_{21} and s. In the present copolymerization k_{21} substantially means k_{121} because homopropagation of M_2 monomer is negligible.

Using the relationship between k_p and f_1 in Fig. 5, we have attempted to evaluate k_{21} and s according to the nonlinear least-squares method. The best curve fitting calculation gave the following results:

$$k_{21} = k_{121} = 19\ \mathrm{L \cdot mol^{-1} \cdot s^{-1}}; \qquad s = k_{211}/k_{111} = 3{,}1 \cdot 10^{-2}$$

The solid line in Fig. 5 was calculated using these values.

Using these data and the rate constant of homopolymerization of M_1 monomer, rate constants of five propagations for the penultimate model in the copolymerization of **1** (M_1) and **2** (M_2) were determined as follows:

$$-M_1M_1^{\bullet} + M_1 \xrightarrow{k_{111} = 140\ \mathrm{L \cdot mol^{-1} \cdot s^{-1}}} -M_1M_1M_1^{\bullet} \quad (15)$$

$$-M_2M_1^{\bullet} + M_1 \xrightarrow{k_{211} = 4{,}3\ \mathrm{L \cdot mol^{-1} \cdot s^{-1}}} -M_2M_1M_1^{\bullet} \quad (16)$$

$$-M_1M_1^{\bullet} + M_2 \xrightarrow{k_{112} = 778\ \mathrm{L \cdot mol^{-1} \cdot s^{-1}}} -M_1M_1M_2^{\bullet} \quad (17)$$

$$-M_2M_1^{\bullet} + M_2 \xrightarrow{k_{212} = 24\ \mathrm{L \cdot mol^{-1} \cdot s^{-1}}} -M_2M_1M_2^{\bullet} \quad (18)$$

$$-M_1M_2^{\bullet} + M_1 \xrightarrow{k_{121} = 19\ \mathrm{L \cdot mol^{-1} \cdot s^{-1}}} -M_1M_2M_1^{\bullet} \quad (19)$$

Thus, the reactivity of propagating radical derived from **1** is strongly depressed by the penultimate unit of **2**. We believe that this remarkable penultimate effect comes from the steric effect due to the highly constrained structure of 1,2-disubstituted **2** monomeric unit and causes a large gap between the k_p values at $f_1 = 0{,}9$ and $f_1 = 1{,}0$.

Using $r_2 = 0{,}01$ and k_{121}, k_{122} was estimated to be 0,19 $\mathrm{L \cdot mol^{-1} \cdot s^{-1}}$ which is twice as large as k_{222} (k_p for homopolymerization of **2**). The reactivity of propagating

radical **5** is enhanced by the penultimate **1** monomeric unit because the terminal radical is free from the steric effect due to the penultimate **2** monomeric unit.

Fukuda et al. suggested that the penultimate effect is more pronounced in the copolymerization with higher tendency toward alternation[5,16]. In fact, a pronounced penultimate effect was observed in the alternating copolymerization of styrene and the diethyl itaconate-$SnCl_4$ complex[18].

However, in order to analyze the penultimate effect more quantitatively, it is necessary to determine separately the concentrations of propagating radicals **4** and **5**, for which the deuterated monomers should be used.

Relationship between k_t and f_1

Fig. 6 shows the relationship between the apparent termination rate constant and the monomer feed composition. The k_t value increases with increasing f_1 and shows a strikingly rapid increase at $f_1 = 1{,}0$. This is because the structure of poly(**1**) greatly

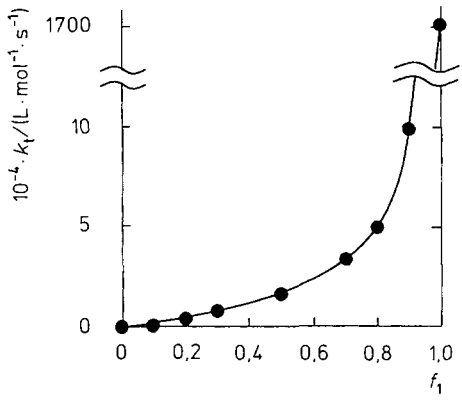

Fig. 6. Relationship between the apparent rate constant (k_t) and f_1 ([**1**]/([**1**] + [**2**]))

differs from those of the resulting copolymers having a highly alternating nature. The difference in the structure of polymers causes the large gap between the diffusion-controlled rate constants of termination, which are mainly dependent on segmental diffusion of propagating polymer chain[19].

The authors are grateful to *Hokko Chemical Industry Co., Ltd.* for the supply of *p-tert*-butoxystyrene.

[1] T. Fukuda, Y.-D. Ma, H. Inagaki, *Macromolecules* **18**, 17 (1985)
[2] S. Iwatsuki, A. Kondo, H. Harashina, *Macromolecules* **17**, 2473 (1984)
[3] T. Kelen, F. Tüdős, D. Braun, W. K. Czerwinski, *Makromol. Chem.* **191**, 1853 (1990)
[4] M. C. Piton, M. A. Winnik, T. P. Davis, K. F. O'Driscoll, *J. Polym. Sci., Part A: Polym. Chem.* **28**, 2097 (1990)

[5] T. Fukuda, Y.-D. Ma, H. Inagaki, *Macromolecules* **24**, 370 (1991)
[6] T. Kelen, F. Tüdős, D. Braun, W. K. Czerwinski, *Makromol. Chem.* **193**, 749 (1992)
[7] T. P. Davis, K. F. O'Driscoll, *J. Polym. Sci., Part C: Polym. Lett.* **27**, 181 (1989)
[8] T. Sato, K. Takahashi, H. Tanaka, T. Ota, *Macromolecules* **24**, 2330 (1991)
[9] T. Sato, S. Kawasaki, M. Seno, H. Tanaka, K. Kato, *Makromol. Chem.* **194**, 2247 (1993)
[10] B. Yamada, M. Fujita, T. Otsu, *Makromol. Chem.* **192**, 1829 (1991)
[11] B. Yamada, M. Kageoka, T. Otsu, *Macromolecules* **24**, 5234 (1991)
[12] M. Yoshioka, A. Matsumoto, T. Otsu, *Polym. J.* **23**, 1249 (1991)
[13] M. Imoto, M. Kinoshita, M. Nishigaki, *Makromol. Chem.* **86**, 212 (1965)
[14] M. Yoshioka, T. Otsu, *Macromolecules* **25**, 559 (1992)
[15] M. S. Matheson, E. E. Auer, E. B. Bevilaqua, E. J. Hart, *J. Am. Chem. Soc.* **73**, 1700 (1951)
[16] K. O'Driscoll, *Makromol. Chem., Macromol. Symp.* **53**, 53 (1992)
[17] J. Schweer, *Makromol. Chem., Theory Simul.* **2**, 485 (1993)
[18] H. Nakamura, M. Seno, H. Tanaka, T. Sato, *Makromol. Chem.* **194**, 1773 (1993)
[19] M. Kamachi, *Makromol. Chem., Suppl.* **14**, 17 (1985)